

Supporting Information

Bloch-type magnetic skyrmions in two-dimensional lattice

Wenhui Du, Kaiying Dou, Zhonglin He, Ying Dai*, Baibiao Huang, Yandong Ma*

School of Physics, State Key Laboratory of Crystal Materials, Shandong University, Shandan
Street 27, Jinan 250100, China

*Corresponding author: daiy60@sina.com (Y.D.); yandong.ma@sdu.edu.cn (Y.M.)

Note 1 : Calculation details of magnetic parameters in spin Hamiltonian

The magnetic parameters are obtained from DFT calculations. The DMI vector D_{ij} for the nearest-neighbor Mn atoms can be expressed as $D_{ij} = d_{\parallel} u_{ij} + d_{\perp} z$ with u_{ij} representing the unit vector pointing from site i to j and z being the out-of-plane unit vector. To obtain the in-plane component d_{\parallel} , the left- and right-hand spin-spiral configurations are considered, as shown in **Fig. 2(a)**. The energy of two spin configurations represented by E_L and E_R can be written as:

$$E_L = E_0 - \frac{3}{2} d_{\parallel} |S|^2 \times 4$$

$$E_R = E_0 + \frac{3}{2} d_{\parallel} |S|^2 \times 4$$

As a result, the in-plane component d_{\parallel} can be obtained by $d_{\parallel} = \frac{E_R - E_L}{12}$.

To obtain J , λ and K_{MCA} , we consider four different spin configurations as displayed in **Fig. S4**. The energy of these different spin configurations can be written as:

$$E_1 = E_0 - 6J|S|^2$$

$$E_2 = E_0 + 2J|S|^2$$

$$E_3 = E_0 - 6J|S|^2 - 6\lambda|S|^2 - 2K_{MCA}|S|^2$$

$$E_4 = E_0 + 2J|S|^2 + 2\lambda|S|^2 - 2K_{MCA}|S|^2$$

Here, E_1 , E_2 , E_3 and E_4 represents the energy of x-FM, x-AFM, z-FM, and z-AFM configurations, respectively. Based on the above formula, magnetic parameters J , λ and K_{MCA} can be obtained.

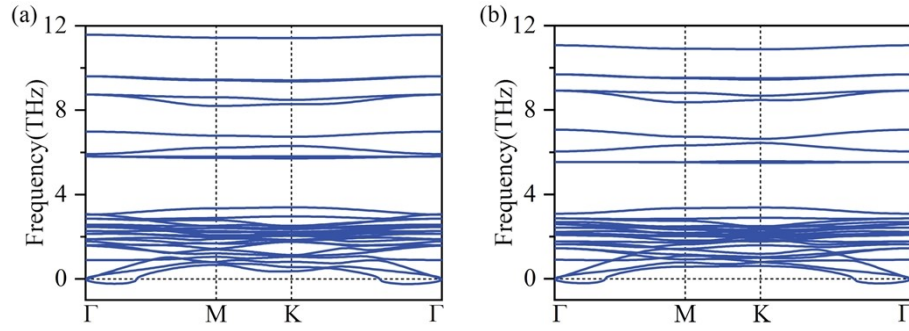


Fig. S1. Phonon spectra of monolayer (a) $\text{MnInP}_2\text{Te}_6$ and (b) $\text{MnTlP}_2\text{Te}_6$. It can be seen that only a tiny negative frequency is observed around the Γ point, suggesting the dynamic stability of monolayer MnXP_2Te_6 .

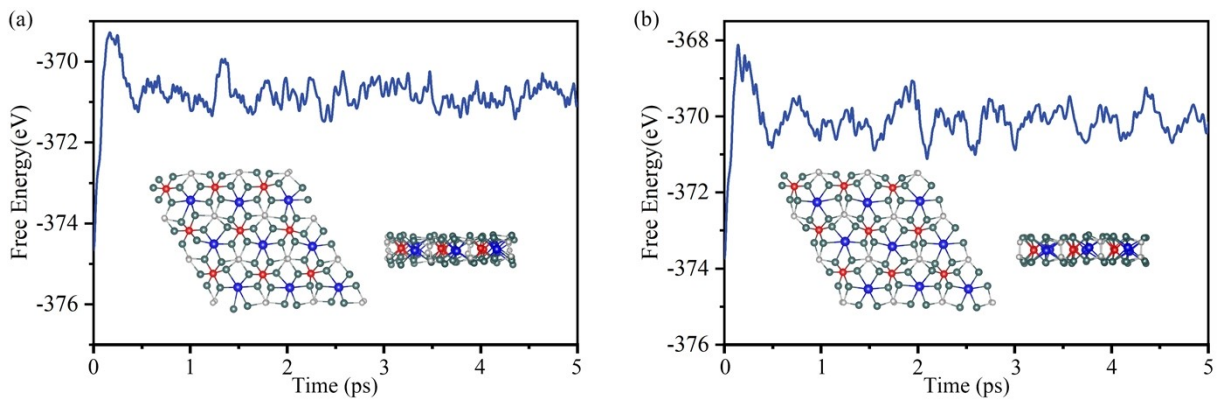


Fig. S2. Variations of total energies with time during the Ab initio molecular dynamics simulations for monolayer (a) $\text{MnInP}_2\text{Te}_6$ and (b) $\text{MnTlP}_2\text{Te}_6$ at 300 K and the corresponding snapshots taken from the end of the simulations. The slight free-energy fluctuations and well-defined structures indicate the thermal stability of monolayer MnXP_2Te_6 .

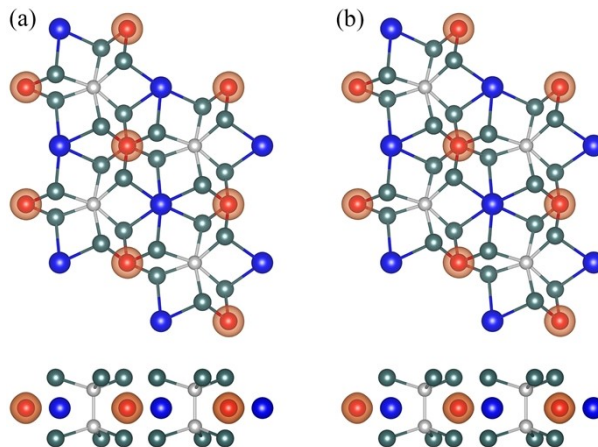


Fig. S3. Spin charge densities of monolayer (a) $\text{MnInP}_2\text{Te}_6$ and (b) $\text{MnTlP}_2\text{Te}_6$.

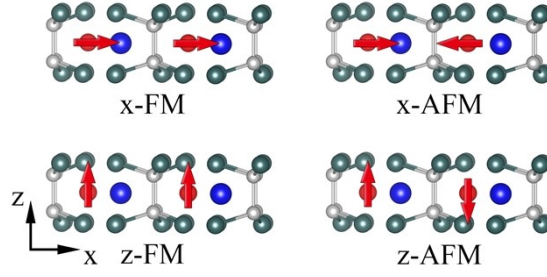


Fig. S4. Four different magnetic configurations used to obtain the magnetic parameters J , λ , and K_{MCA} in monolayer MnXP_2Te_6 .

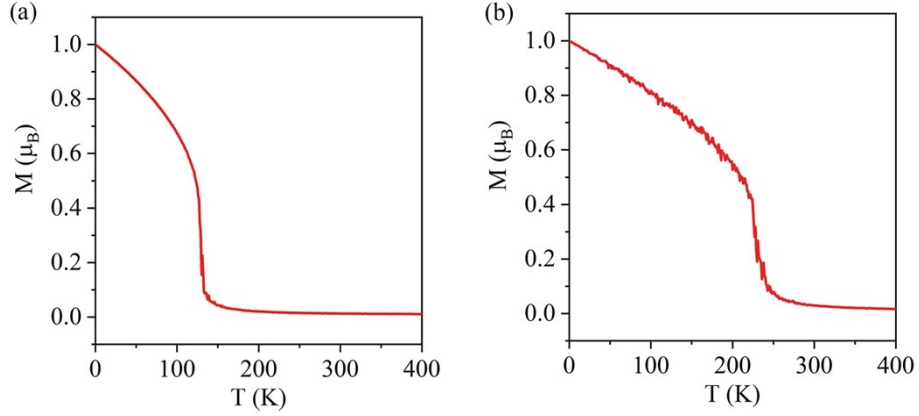


Fig. S5. Average magnetization (M) per formula as a function of temperature (T) of monolayer (a) $\text{MnInP}_2\text{Te}_6$ and (b) $\text{MnTlP}_2\text{Te}_6$ from Monte-Carlo simulations.

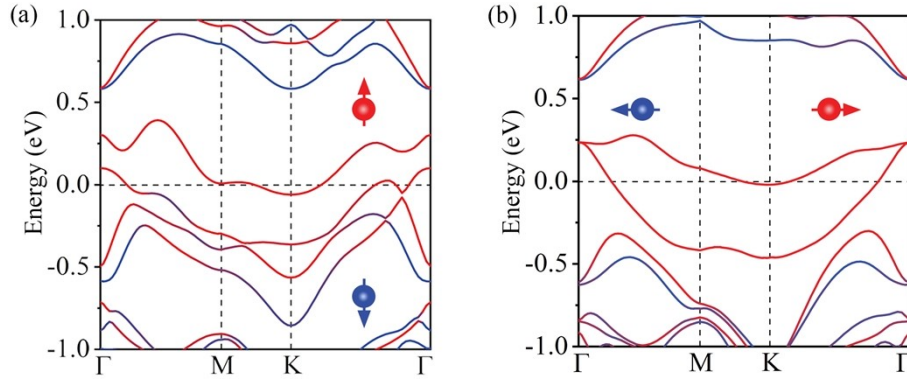


Fig. S6. Spin-polarized band structures of monolayer (a) $\text{MnInP}_2\text{Te}_6$ and (b) $\text{MnTlP}_2\text{Te}_6$ with SOC. The red and blue lines in (a, b) correspond to spin-up and spin-down states, respectively. The Fermi level is set to 0 eV.

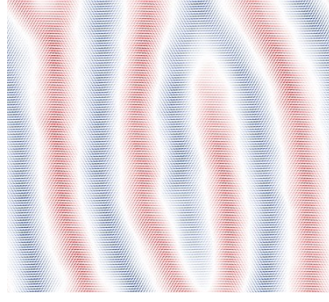


Fig. S7. Spin texture of monolayer $\text{MnTIP}_2\text{Te}_6$ under in-plane magnetic field of 19 mT. It is superimposed by in-plane cycloidal structure and small out-of-plane wavy spin pattern.

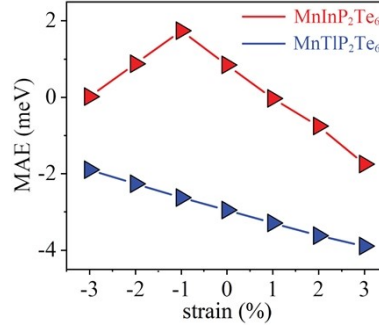


Fig. S8. Magnetic anisotropy energy (MAE) per unit cell of monolayer MnXP_2Te_6 as a function of strain. MAE is defined as the energy difference between the systems with magnetization axis along in-plane ($E_{in-plane}$) and out-of-plane ($E_{out-of-plane}$) directions.

Table S1. Lattice constant a (\AA), magnetic parameters [exchange coupling J (in meV), anisotropic symmetric exchange λ (in meV), magnetocrystalline anisotropy K_{MCA} (in meV), magnetic shape anisotropy K_{MSA} (in meV), single ion anisotropy K (in meV), in-plane DMI d_{\parallel} (in meV)] and magnetic moment m (μ_B) on Mn atom for monolayer MnXP_2Te_6 .

	a	J	λ	K_{MCA}	K_{MSA}	K	d_{\parallel}	m
$\text{MnInP}_2\text{Te}_6$	7.13	10.108	-0.048	1.015	-0.026	0.989	2.873	4.191
$\text{MnTIP}_2\text{Te}_6$	7.20	18.168	-0.955	-0.064	-0.025	-0.089	5.791	4.173

Table S2. Lattice constants a (\AA), magnetic parameters [exchange coupling J (in meV), anisotropic symmetric exchange λ (in meV), magnetocrystalline anisotropy K_{MCA} (in meV), magnetic shape anisotropy K_{MSA} (in meV), single ion anisotropy K (in meV), in-plane DMI d_{\parallel} (in meV)] and

magnetic moments m (μ_B) on Mn atom for monolayer MnInP₂Te₆ under various strains.

MnInP ₂ Te ₆	a	J	λ	K_{MCA}	K_{MSA}	K	d_{\parallel}	m
-3%	6.92	5.197	0.205	-0.567	-0.028	-0.595	1.409	4.254
-2%	6.99	5.965	0.340	-0.114	-0.027	-0.141	1.746	4.232
-1%	7.06	8.169	0.342	0.739	-0.027	0.712	2.293	4.207
0%	7.13	10.108	-0.048	1.015	-0.026	0.989	2.873	4.191
1%	7.20	11.475	-0.510	1.519	-0.025	1.494	3.653	4.178
2%	7.27	12.622	-0.946	2.109	-0.024	2.085	4.600	4.175
3%	7.34	13.321	-1.202	1.881	-0.024	1.857	5.517	4.172

Table S3. Lattice constants a (Å), magnetic parameters [exchange coupling J (in meV), anisotropic symmetric exchange λ (in meV), magnetocrystalline anisotropy K_{MCA} (in meV), magnetic shape anisotropy K_{MSA} (in meV), single ion anisotropy K (in meV), in-plane DMI d_{\parallel} (in meV)] and magnetic moments m (μ_B) on Mn atom for monolayer MnTlP₂Te₆ under various strains.

MnTlP ₂ Te ₆	a	J	λ	K_{MCA}	K_{MSA}	K	d_{\parallel}	m
-3%	6.99	19.700	-0.485	-0.416	-0.027	-0.443	4.095	4.184
-2%	7.06	19.600	-0.688	-0.178	-0.027	-0.205	4.753	4.177
-1%	7.13	19.111	-0.850	-0.053	-0.026	-0.079	5.362	4.172
0%	7.20	18.168	-0.955	-0.064	-0.025	-0.089	5.791	4.173
1%	7.27	17.056	-1.050	-0.114	-0.024	-0.138	6.035	4.174
2%	7.35	15.969	-1.154	-0.137	-0.024	-0.161	6.106	4.180
3%	7.42	14.909	-1.248	-0.126	-0.023	-0.149	6.088	4.189